NASA TECHNICAL MEMORANDUM

NASA TM X-1053

NASA TM X-1053

FLIGHT MEASUREMENTS OF REENTRY HEATING AT HYPERBOLIC VELOCITY (PROJECT FIRE)

by Richard C. Dingeldein

Langley Research Center

Langley Station, Hampton, Va.

NATIONAL AERONAUTICS AND SPACE ADMINISTRATION • WASHINGTON, D. C. • JANUARY 1965

FLIGHT MEASUREMENTS OF REENTRY HEATING AT HYPERBOLIC VELOCITY (PROJECT FIRE)

R. C. Dingeldein

Langley Research Center
Hampton, VA

JAN 65

FLIGHT MEASUREMENTS OF REENTRY HEATING AT HYPERBOLIC VELOCITY (PROJECT FIRE) (U)

By Richard C. Dingeldein

Langley Research Center
Langley Station, Hampton, Va.

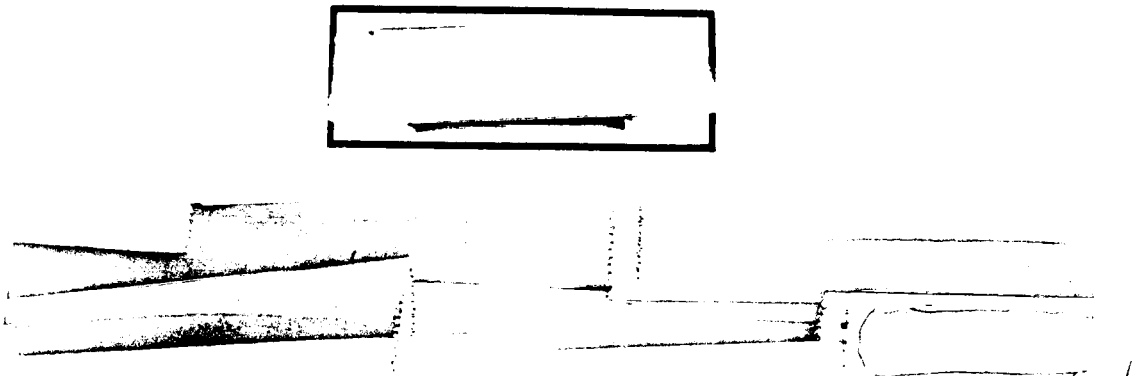

NATIONAL AERONAUTICS AND SPACE ADMINISTRATION

FLIGHT MEASUREMENTS OF REENTRY HEATING AT HYPERBOLIC VELOCITY (PROJECT FIRE)* **

By Richard C. Dingeldein
Langley Research Center

SUMMARY

The initial Project Fire reentry experiment has provided flight measurements of reentry heating at a velocity of nearly 38 000 feet per second. Reduction and analysis of the data are not complete; however, pertinent results of the major onboard experiments are presented in this status report along with comparisons afforded by available theory.

INTRODUCTION

Project Fire is a flight research investigation undertaken by the National Aeronautics and Space Administration to provide measurements of reentry heating at large scale on a blunt body entering the earth's atmosphere at a velocity of over 37 000 feet per second. The resulting data are expected to provide a valuable check of theoretical prediction methods and the results of ground facilities experiments and their extrapolation.

The project provides for the launch along the Eastern Test Range of a 3900-pound powered spacecraft mounted atop an Atlas D launch vehicle. After separation from the launch vehicle and orientation to the inertial reentry attitude, the spacecraft coasts to a point approximately 4000 international nautical miles downrange. Here, at an altitude of about 1×10^6 feet, the reentry stage is spin stabilized and the Antares-II motor is separated from the guidance components and ignited to provide a velocity increment of nearly 17 000 feet per second. This produces a reentry speed of over 37 000 feet per second. The reentry package is then separated from the spent motor. The latter is subsequently tumbled to increase its aerodynamic drag.

The Fire reentry package permits measurement of the combined effects of convective and radiative heating (referred to as total heating) using metal calorimeters extensively instrumented with thermocouples. Direct measurements of gas radiation are provided by onboard radiometers. The reentry package is

*Paper presented at a closed session of the Entry Technology Conference held by the American Institute of Aeronautics and Astronautics, Williamsburg/Hampton, Virginia, Oct. 12-14, 1964. Since the AIAA has no provision for publishing classified material, this paper is being given limited distribution by the NASA.

constructed with a layered heat shield, which facilitates making measurements from these sensors in three distinct periods during the reentry heating pulse of approximately 40 seconds duration. Afterbody temperatures and static pressures are also measured, along with the outputs of orthogonally mounted rate gyros and linear accelerometers. Upon emergence from telemetry blackout, the data recorded onboard during the reentry heating period are continuously replayed until splash. No recovery of the reentry package was planned. Provision has been made for a total of two launches.

On April 14, 1964, at 2142:25.536 G.M.T., the Fire I vehicle was launched from Cape Kennedy, Florida. The complex series of events required to carry out the reentry experiments took place almost exactly as planned. The total-heating sensors and the radiometers operated properly and a substantial amount of data was obtained. However, a deterioration of the telemetry system used for postblackout playback of the data resulted in numerous periodic dropouts which necessitated time-consuming manual data reduction. Also, the effect on the interpretation of the Fire data of a severe reentry-package motion which began approximately halfway through the reentry has not yet been assessed. This paper should therefore be considered as a status report of the Fire I results. Data obtained from the principal experiments carried aboard the Fire I reentry package are presented along with comparisons afforded by available theory.

SYMBOLS

S	projected area, square feet
C_D	drag coefficient
h	altitude, feet
l	afterbody length, feet
q_{cal}	heating rate defined by temperature time history of beryllium calorimeter, watts per square centimeter
q_c	convective heating rate, watts per square centimeter
q_r	radiative heating rate, watts per square centimeter
V	velocity, feet per second
W	weight, pounds
x	distance measured rearward from beginning of afterbody, feet
T	equilibrium stagnation absolute temperature, degrees Rankine
a	absorptivity

γ flight-path angle measured with respect to the local horizontal, degrees

ρ_o sea-level atmospheric density, slugs per cubic foot

ρ_∞ free-stream density, slugs per cubic foot

RESULTS AND DISCUSSION

Reentry Conditions

The altitude and velocity time histories for the Fire I reentry are shown in figure 1. At the beginning of the reentry, which is arbitrarily defined as the conditions existing at an altitude of 400 000 ft, the aerodynamic velocity was 37 971 ft/sec and the reentry angle was -14.6°. These curves have been obtained from the C-band radar tracking data and a computer simulation of the reentry during the C-band beacon blackout period. The simulation utilized atmospheric characteristics obtained from soundings conducted from Ascension Island a few hours after reentry which gave results that were very close to the 1962 U.S. Standard Atmosphere (ref. 1). The ballistic number of the reentry package $\left(W/C_D S\right)$ remained fairly constant at a value of approximately 32.5 lb/sq ft during reentry. The velocity of the reentry package was greater than the nominal Apollo reentry speed of approximately 35 500 ft/sec for the first 25 sec of the reentry.

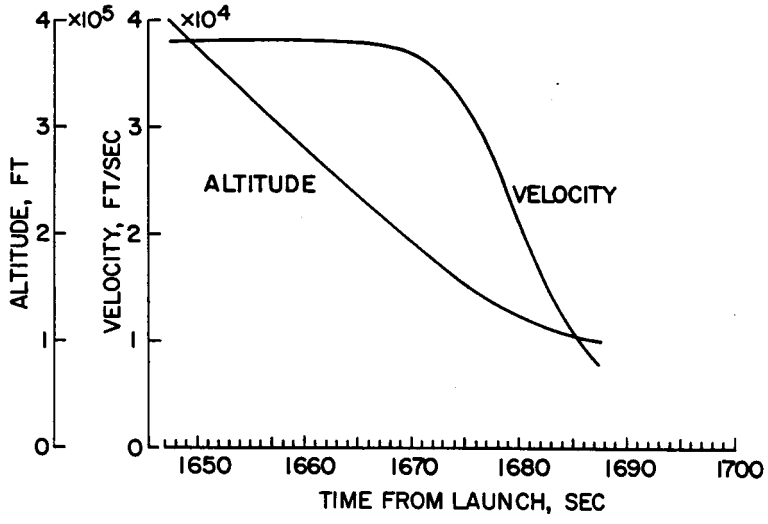

Figure 1.- Reentry velocity and altitude time histories.

Reentry Package

The front, side, and rear views of the Fire reentry package are shown in figure 2. At the start of reentry, the reentry package weighed 184 lb and was 26.44 in. in diameter. The blunt front face consisted of six separate heat-shield layers. The first, third, and fifth layers were solid beryllium calorimeters having a surface finish of 8 μin. (root-mean-square value). Forty-eight thermocouples were installed in each beryllium calorimeter layer at the locations designated in figure 2 and at depths of 0.010, 0.070, 0.130, and

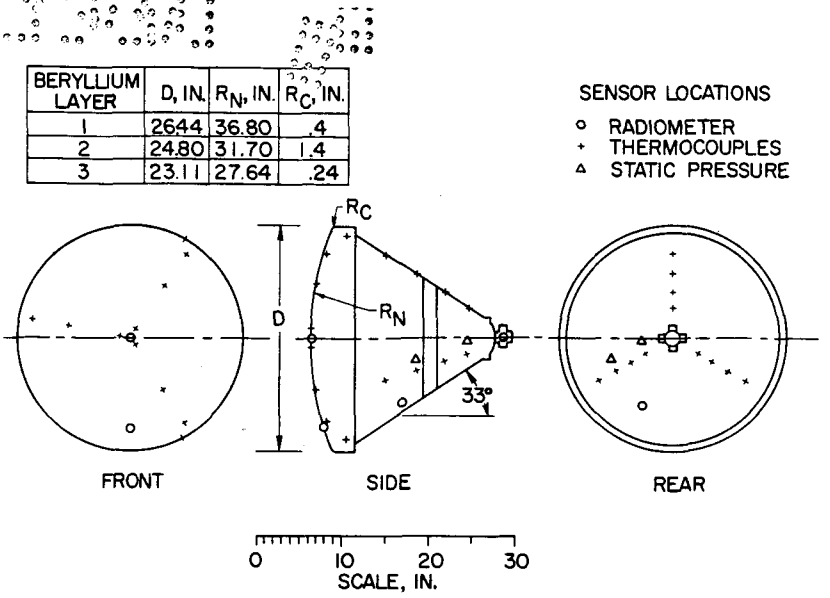

Figure 2.- Reentry package geometry and sensor locations.

0.200 in. from the heated surface to measure the temperature time histories resulting from convective heating and absorbed radiation. The second, fourth, and sixth layers consisted of a high-density, high-strength phenolic-asbestos laminate. The second and fourth layers served to protect the beryllium calorimeters just behind them, and were mechanically ejected at preselected times during reentry to expose the succeeding cool beryllium layers and uncontaminated optical windows. The last ablation layer served as the final protection for the reentry package after the third beryllium calorimeter had melted off. This novel layered heat shield permitted obtaining forebody reentry heating measurements during three distinct portions of the 40-sec heat pulse. The projected diameter and nose and corner radii of each of the three beryllium calorimeter layers are given in figure 2. During the second data period, the geometry is the same as that for the Apollo command module.

Radiometers were installed to permit measuring the gas radiance at the nominal stagnation point at the center of the heat shield, at a point offset approximately 16° along the spherical heat-shield face, and at a location on the afterbody. Total radiation was measured at all three locations in the wavelength range from 0.23μ to 4.5μ transmitted by the fused-quartz optical windows. In addition, a rocking-grating monochrometer scanned radiation between 0.23μ and 0.60μ 10 times a second with a resolution of 50 Å. During the calorimeter data periods, the stagnation-point and offset radiometers measured radiation uncontaminated by ablation products.

Temperatures were measured at 12 locations on the afterbody corresponding to 4 longitudinal stations. The sensors consisted of thermocouples embedded in peripherally insulated gold calorimeter slugs having a high emissivity coating and set flush with the surface. At two of these longitudinal stations, static pressures were also measured.

The turnstile-shaped appendage at the afterbody apex is the antenna for the C-band beacon installed to facilitate radar tracking. There were two VHF telemetry systems onboard with antennas located in the band shown in the side view of figure 2. One telemetry system broadcast the reentry package data in real time; the other broadcast the data stored on a 45-second recorded loop of tape. Upon emergence from VHF blackout, the record and erase functions of the tape recorder were disabled. This feature permitted continuous replaying of the data obtained during the blackout period until splash occurred. No recovery of the reentry package was planned.

Motions of the reentry package were sensed by a three-axis system of accelerometers and rate gyros.

The data presented in this paper consist of the temperature time histories and deduced calorimeter heat flux corresponding to measurements made adjacent to the nominal stagnation point, the total radiation measured at the stagnation point during the periods of good transmission properties of the exposed optical window, afterbody temperature time histories, and the radio blackout experienced by the VHF telemetry and the C-band beacon broadcast.

Reentry Telemetry and Events

The major events occurring during the Fire I reentry are shown in figure 3 along with an analog representation of the telemetry received during this period. The events noted in terms of the elapsed time from launch in seconds are the separation of the reentry package (R/P) from the spent velocity package, the start of the reentry arbitrarily defined at an altitude of 400 000 ft, the points at which VHF communications were lost due to the plasma sheath and later regained, the point at which an abrupt motion of the reentry package (which had a very smooth separation from the velocity package) was noted, the start of the onboard timer which initiated the subsequent ejections of the first and second ablation layers to expose the second and third beryllium calorimeter layers, and the point at which the record and erase heads of the onboard tape recorder were disabled to permit subsequent continuous replays of the stored data until splash. It should be noted that the reentry-package motions are presently being analyzed in order to better assess their effect on the succeeding data. There is substantial

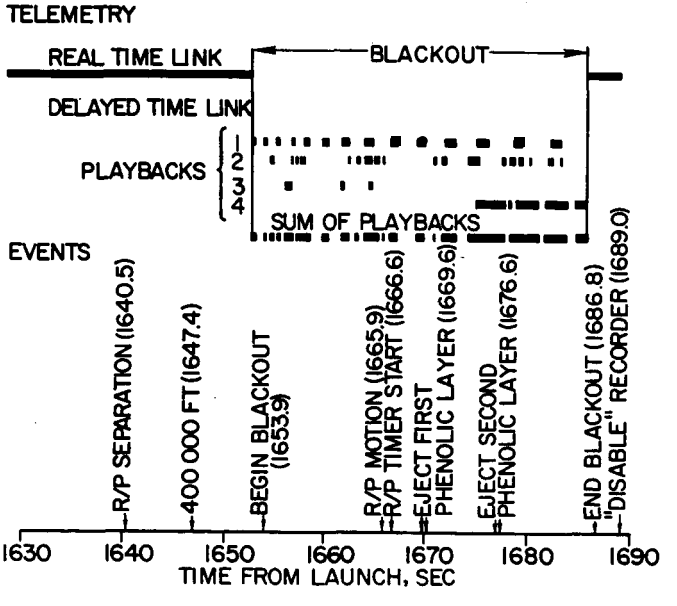

Figure 3.- Reentry telemetry and events.

evidence to show that the motions were initiated by the near passage of the spent velocity package.

In the upper portion of figure 3, the periods during which telemetry was received from the real-time broadcast and from the delayed-time data playbacks are shown. The VHF blackout is discussed subsequently, but it is noted here that the blackout appearance and disappearance occurred abruptly and without warning. Portions of the first four delayed-time-broadcast data-playback cycles received have been inserted into the real-time reference. A large loss in the delayed-time telemetry signal strength was originally noted following the spinup of the reentry stage prior to ignition of the Antares-II motor. The resulting data dropouts can be roughly correlated with the aspect angles of the reentry package and the telemetry antenna patterns. Portions of the first three playback cycles which can be described as somewhat "noisy" were obtained by the Ascension telemetry facility, and the latter part of the fourth playback cycle was recorded by a range telemetry ship. A summation of the telemetry received during the blackout period indicated that approximately two-thirds of the data could be extracted. The data dropouts necessitated a manual reduction of the data rather than the computing machine operation originally planned. Although deteriorated telemetry was received, planned redundancies in respect to the number of data playbacks and dispersion of receiving equipment have nevertheless resulted in obtaining a considerable amount of research information.

Reentry Data

Calorimeter temperature time histories.- The effect of the degraded delayed-time telemetry on the temperature time histories obtained from thermocouples located near the center of the three beryllium calorimeter layers is shown in the sample data presented in figure 4. These data, which are normally commutated at the rate of 10 samples/sec, are presented for thermocouple junctions located closest (0.010 in.) and farthest (0.200 in.) from the heated calorimeter surface. In the interest of clarity, the time histories obtained at two intermediate depths have not been included. Prior to VHF blackout, the data are characterized by relatively low scatter, approximately $\pm 20^{\circ}$ R, and by no dropouts. From the onset of VHF blackout, use of the delayed-time data is seen to result in numerous dropouts and greatly increased scatter. Inasmuch as several reasonable fairings of the resulting data points can be obtained, the subsequent analysis of the temperature time histories to calculate the corresponding heat flux to which the calorimeters were exposed is presented as the band defined by the various fairings of the experimental data. An interesting aspect of figure 4(b) is the evidence that the layers of ablation material subsequently ejected to expose the second and third beryllium calorimeters did provide the desired protection in that the initial temperatures indicate that each of the data periods began with a cool calorimeter. The first and third calorimeter layers were 0.120 in. thick, with bosses extending the thickness to 0.200 in. at the thermocouple locations. The boss dimensions were selected to insure one-dimensional heat flow at the thermocouple locations. The second beryllium calorimeter was uniformly 0.200 in. thick. The temperature time histories for the first and third beryllium calorimeter layers have been terminated

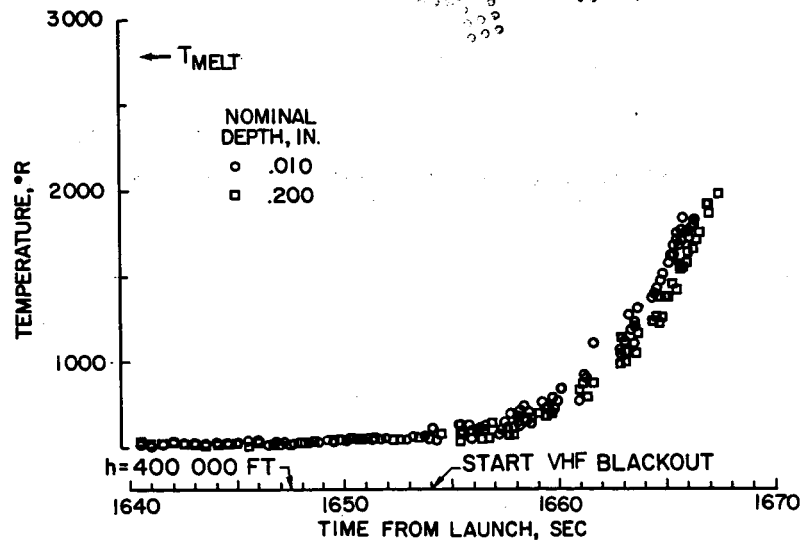

(a) First calorimeter data period.

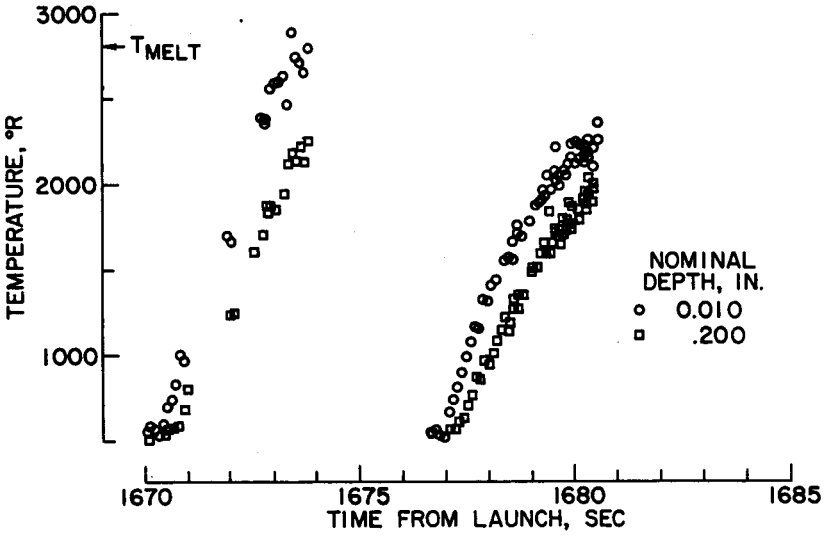

(b) Second and third calorimeter data periods.

Figure 4.- Measured temperature time histories.

at the time the thinner portions of the calorimeter approached surface melting. A subsequent rigorous three-dimensional analysis of the possible errors due to heat flowing into the bosses has indicated a maximum error of 100° R at the end of the first calorimeter data period. The calorimeter flux deduced from the temperature time histories, which is presented later, includes this correction.

Stagnation total radiometer.- The radiative flux measured by the total radiometer located at the center of the heat shield is presented in figure 5 as a function of the free-stream density ratio. Although the radiometer

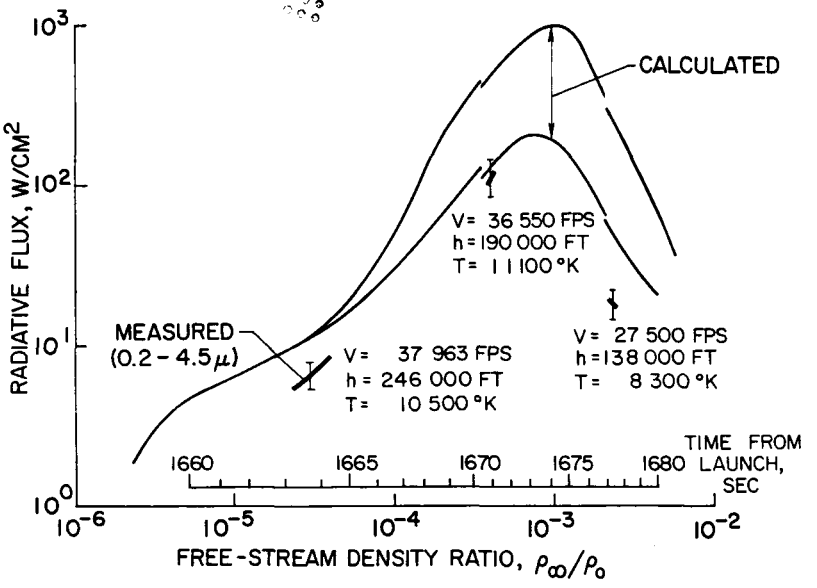

Figure 5.- Stagnation-point total-radiometer measurements.

measured radiation levels throughout the reentry, the data are presented only for those periods prior to incipient surface melting of the exposed optical window. The velocity, altitude, and the estimated equilibrium gas temperatures at the stagnation point (ref. 2) are given at the end of each data period. The estimated accuracy of the data is also shown. Corrections have been applied for the optical window transmission properties and window emittance. These corrections are relatively small, averaging less than 1 percent. For reference purposes, a range of stagnation-point radiative heat fluxes calculated for the Fire reentry package trajectory using different methods is also shown. The lower curve is based on equilibrium radiation calculations using the absorption coefficients of reference 3; the upper curve on the method of Kivel and Bailey (ref. 4). The nonequilibrium contributions have been estimated from the hypervelocity ballistic range measurements conducted at the Ames Research Center (ref. 5) extrapolated to the Fire I reentry speed of 11.56 km/sec, with empirical corrections for collision-limiting and truncation effects applied by using the data of reference 6. During the first data period, where nonequilibrium radiation dominates $\left(\frac{\rho_\infty}{\rho_o} \leqq 4 \times 10^{-5}\right)$, the Fire results indicate radiative flux levels between one-half and two-thirds the estimated values. During the second data period, due to the reentry package motions mentioned earlier, the radiometer measured oscillating radiation levels. Analysis of the onboard inertial sensors indicates that the period is in general agreement with the calculated angle-of-attack excursions and that the peak radiation levels have probably been measured at angles of attack of 5° or less. The radiometer flux plotted for the second data period represents a fairing of the measured peak values. During this period $\left(\frac{\rho_\infty}{\rho_o} \approx 4 \times 10^{-4}\right)$ the Fire I values are approximately

75 percent of the lower theoretical predictions during the last data period, the measurements are approximately 40 percent of the lower prediction.

Calorimeter flux.- Fairings of the measured temperature time histories for the four thermocouple depths at a location near the center of each of the beryllium calorimeter layers have been used to define the calorimeter flux by solving the differential heat flow equation using temperature-dependent-material properties. The resulting flux is approximately equal to the sum of the convective heating rate and the absorbed radiative heating rate. The calorimeter flux thus determined has been corrected for surface emission, which is extremely small. The measured flux for the three calorimeter data periods is shown by the solid bands in figure 6. For reference purposes, calculations of the calorimeter flux using Cohen's method for predicting convective heating (ref. 7) and absorbed radiation based on the predicted fluxes given in figure 5 are also presented. An absorption of 0.5 has been applied to the calculated radiative flux. This factor was obtained from tests of calorimeter specimens conducted in the range of wavelengths from 0.26μ to 2.1μ and represents a weighted average based on the spectral distribution of the radiance predicted by using the method of reference 3. The results obtained from the Fire reentry generally fall within or very close to the theoretical predictions. The theoretical estimates are for zero angle of attack. Consideration of the body motions estimated during the second data period and convective-heat-transfer data obtained on the Apollo command module shape (ref. 8) indicate that the average convective heating rate near the center of the heat shield might be reduced by as much as 10 percent from the zero-angle-of-attack value.

Also shown in figure 6 are points representing the sum of convective and absorbed radiative heating rates obtained from detailed analyses[1] of the reentry package flow fields and associated heating rates based on the nominal Fire reentry

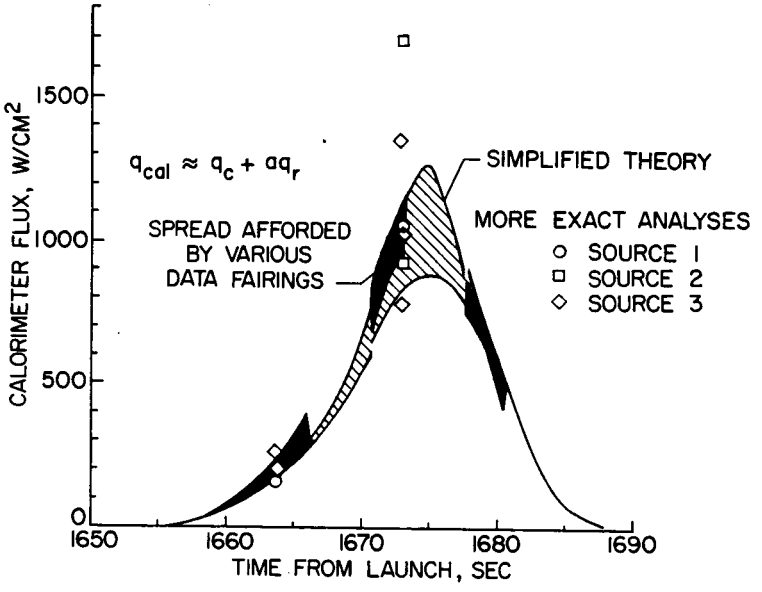

Figure 6.- Heat flux deduced from beryllium calorimeter temperatures measured adjacent to the stagnation point.

[1]These analyses are identified as follows:
Source 1: Philco Corporation (Contract NAS 1-3419).
Source 2: General Electric Company (Contract NAS 1-3418).
Source 3: Lockheed Missiles & Space Company (Contract NAS 1-3417).

conditions ($V = 37\,335$ ft/sec, $h = 400\,000$ ft, $\gamma = -15^\circ$). These studies, which largely represent the application of different analytical methods, generally confirm the previously discussed calorimeter flux predictions and are in the range of the experimental results. The two highest points shown at 1673 sec include radiation estimated in the vacuum ultraviolet region. At the aforementioned time, the highest point (source 2) includes absorbed radiation in the range of wavelengths from 0.05μ to 10μ. The result from source 2 located inside the theory boundaries represents the same solution when all radiation below 0.16μ is ignored. The results from source 3 plotted at 1664 sec are of interest in that the higher of the two points includes vorticity effects on the convective heating. The existence of vorticity effects at the low Reynolds numbers representative of the early part of the reentry may tend to explain the somewhat higher flux indicated by the calorimeter measurements compared with the plotted theoretical boundaries which did not consider these effects. The calorimeter measurements can be considered as indicative of the total heating effects at the Fire reentry velocity. This heating environment can be predicted with fairly good accuracy with the use of available methods. The differences between the measured calorimeter fluxes shown in figure 6 and the measured radiative flux given in figure 5 and corrected for the proper calorimeter absorption factors represents the sum of the actual convective heating rate and the radiation absorbed at wavelengths not transmitted by the optical windows. Obtaining calorimeter absorption factors at much lower wavelengths than the present limit of 0.26μ will greatly assist in interpreting the calorimeter data.

Afterbody temperatures.- The temperature time histories measured at four stations on the reentry package afterbody are plotted in figure 7. Also shown are predictions based on a calculated stagnation-point convective heating rate (ref. 7) for zero angle of attack and for a heating distribution estimated to apply at the point when the maximum flux occurs. Despite the effects of the body motions, which have not been estimated, there is rough agreement between the measurements and the estimated temperatures, with the measurements generally indicating lower maximum temperatures. Since the effects of the body motions, which would be expected to influence the afterbody heating, have not been assessed, the local heating fluxes deduced from the measured data have not been presented. They generally range from 12 to 22 W/cm^2 or between 2 and 4 percent of the estimated stagnation-point convective heating rate. The data generally indicate that there are no gross unexpected effects.

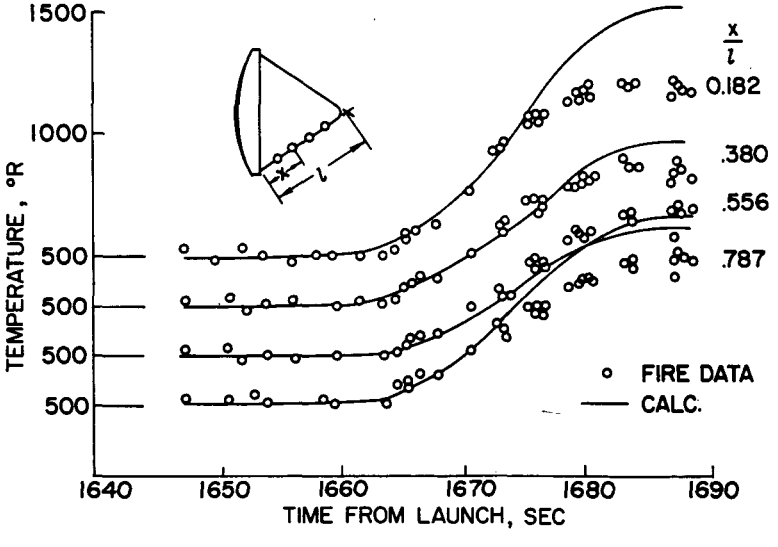

Figure 7.- Afterbody temperatures.

Radio-signal attenuation.- A plot of empirical boundaries below which VHF and C-band radio signal blackout have been experienced in ballistic reentries such as provided by Project Mercury and Project RAM is given in figure 8. The empirical boundaries were originally presented in reference 9. Superimposed on the plot is the Fire I reentry trajectory, along with points designating the altitudes and velocities at which VHF and C-band blackout and emergence from blackout were noted. The usual tracking problems attendant to reacquisition of the C-band beacon prevented establishing the point at which this signal emerged from blackout. The available Fire I results, however, serve to confirm the previous empirical boundaries and have effectively extended them to a velocity of 38 000 ft/sec.

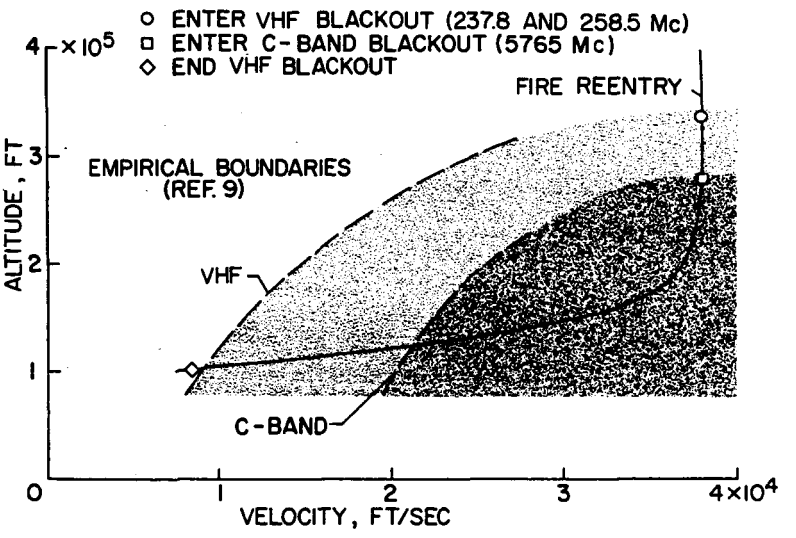

Figure 8.- Radio-signal attenuation.

CONCLUDING REMARKS

The initial Fire reentry experiment has provided flight measurements of reentry heating at a velocity of nearly 38 000 feet per second. Although some deteriorated telemetry was received, planned redundancies in respect to provision for multiple receivers and repeated data playbacks have resulted in obtaining a considerable amount of research information. Reduction and analysis of the Fire I data, including the effect of body motions experienced halfway through the reentry, are not complete at the time of this writing. However, the following remarks are indicated with respect to the results presented in this paper:

Early in the reentry, where nonequilibrium radiation is dominant, the stagnation-point total radiative flux measured between 0.23 and 4.5 microns was approximately two-thirds of the predicted values based on available ground-facility data. In the two data periods later in the reentry, the measured radiative flux was also less than predicted values.

The total heating fluxes defined by the stagnation thermocouple locations in the beryllium calorimeter layers are shown to lie within the latitude afforded by current prediction methods. With estimates of contributions in the vacuum ultraviolet region omitted, the predictions agree rather closely with the band defined by the Fire I measurements.

The afterbody temperature time histories exhibit no unexpected trends. The measured maximum temperatures are generally lower than those calculated for comparison purposes assuming zero angle of attack.

The radio-signal attenuation experienced at VHF and C-band frequencies confirm the previously defined empirical boundaries and have extended the experimental coverage to a velocity of 38 000 feet per second.

Langley Research Center,
National Aeronautics and Space Administration,
Langley Station, Hampton, Va., October 14, 1964.

REFERENCES

1. Anon.: U.S. Standard Atmosphere, 1962. NASA, U.S. Air Force, and U.S. Weather Bureau, Dec. 1962.

2. Ziemer, Richard W.: Extended Hypervelocity Gas Dynamic Charts for Equilibrium Air. STL/TR-60-0000-09093 (Contract No. AF 04(647)-309), Space Technol. Lab., Inc., Apr. 14, 1960.

3. Meyerott, R. E.; Sokoloff, J.; and Nicholls, R. A.: Absorption Coefficients of Air. AFCRC-TR-59-296, U.S. Air Force, Sept. 1959.

4. Kivel, B.; and Bailey, K.: Tables of Radiation From High Temperature Air. Res. Rept. 21 (Contracts AF 04(645)-18 and AF 49(638)-61), AVCO Res. Lab., Dec. 1957.

5. Page, William A.; and Arnold, James O.: Shock-Layer Radiation of Blunt Bodies at Reentry Velocities. NASA TR R-193, 1964.

6. Allen, R. A.; Rose, P. H.; and Camm, J. C.: Non-Equilibrium and Equilibrium Radiation at Super-Satellite Re-Entry Velocities. Paper No. 63-77, Inst. Aerospace Sci., Jan. 1963.

7. Cohen, Nathaniel B.: Boundary-Layer Similar Solutions and Correlation Equations for Laminar Heat-Transfer Distribution in Equilibrium Air at Velocities up to 41,100 Feet Per Second. NASA TR R-118, 1961.

8. Jones, Robert A.: Measured Heat-Transfer and Pressure Distributions on the Apollo Face at a Mach Number of 8 and Estimates for Flight Conditions. NASA TM X-919, 1964.

9. Sims, Theo E.: Langley Reentry Communications Program. Proceedings of the NASA Conference on Communicating Through Plasmas of Atmospheric Entry and Rocket Exhaust. NASA SP-52, 1964, pp. 1-6.